ADVANCED MATERIALS
www.advmat.de

Observation of Superconducting Collective Modes from Competing Pairing Instabilities in Single-Layer $NbSe_2$

*Wen Wan, Paul Dreher, Daniel Muñoz-Segovia, Rishav Harsh, Haojie Guo, Antonio J. Martínez-Galera, Francisco Guinea, Fernando de Juan, and Miguel M. Ugeda**

In certain unconventional superconductors with sizable electronic correlations, the availability of closely competing pairing channels leads to characteristic soft collective fluctuations of the order parameters, which leave fingerprints in many observables and allow the phase competition to be scrutinized. Superconducting layered materials, where electron–electron interactions are enhanced with decreasing thickness, are promising candidates to display these correlation effects. In this work, the existence of a soft collective mode in single-layer $NbSe_2$, observed as a characteristic resonance excitation in high-resolution tunneling spectra is reported. This resonance is observed along with higher harmonics, its frequency $\Omega/2\Delta$ is anticorrelated with the local superconducting gap Δ, and its amplitude gradually vanishes by increasing the temperature and upon applying a magnetic field up to the critical values (T_C and H_{C2}), which sets an unambiguous link to the superconducting state. Aided by a microscopic model that captures the main experimental observations, this resonance is interpreted as a collective Leggett mode that represents the fluctuation toward a proximate *f*-wave triplet state, due to subleading attraction in the triplet channel. These findings demonstrate the fundamental role of correlations in superconducting 2D transition metal dichalcogenides, opening a path toward unconventional superconductivity in simple, scalable, and transferable 2D superconductors.

1. Introduction

In the Migdal–Eliashberg theory[1,2] of superconductivity, electron–phonon coupling is responsible for the attraction that binds Cooper pairs together in the standard s-wave channel. In superconductors with significant electronic correlations, however, the Coulomb repulsion can be detrimental for pairing and other mechanisms need to be invoked to explain the emergence of "unconventional" superconductivity, which often occurs with different pairing symmetry in the spin or orbital sectors. Several classes of correlated electron systems such as the cuprates[3–10], iron-pnictides[11–16], iron-chalcogenides[17–19], and several heavy-fermion compounds[20,21], have been identified as unconventional superconductors and more recently, superconductivity with unconventional features has also been identified in twisted bilayer graphene (TBLG).[22] The different experimental complexities to produce and probe these materials make

W. Wan, P. Dreher, D. Muñoz-Segovia, R. Harsh, F. Guinea, F. de Juan, M. M. Ugeda
Donostia International Physics Center (DIPC)
Paseo Manuel de Lardizábal 4, San Sebastián 20018, Spain
E-mail: mmugeda@dipc.org

H. Guo, A. J. Martínez-Galera
Departamento de Física de la Materia Condensada
Universidad Autónoma de Madrid
Madrid E-28049, Spain

A. J. Martínez-Galera
Instituto Nicolás Cabrera
Universidad Autónoma de Madrid
Madrid E-28049, Spain

F. Guinea
Instituto Madrileño de Estudios Avanzados en Nanociencia (IMDEA-Nanociencia)
C/Faraday 9, Madrid E-28049, Spain

F. de Juan, M. M. Ugeda
Ikerbasque
Basque Foundation for Science
Bilbao 48013, Spain

M. M. Ugeda
(CSIC-UPV-EHU)
Paseo Manuel de Lardizábal 5, San Sebastián 20018, Spain

The ORCID identification number(s) for the author(s) of this article can be found under https://doi.org/10.1002/adma.202206078.

DOI: 10.1002/adma.202206078

the study of their unconventional superconductivity a formidable problem.

In this arena, transition metal dichalcogenides (TMD) are promising candidates to provide an alternative route to unconventional superconductivity. Electronic correlations are intrinsically present in this family of layered materials, which manifest in various ways such as in Mott phases,[23] magnetic order,[24–26] charge/spin density waves,[27] quantum spin liquids,[28] and superconductivity.[22,27,29–34] Furthermore, in two dimensions, electron–electron interactions are markedly enhanced due to reduced screening, which can enable non-phononic Cooper pairing mechanisms. Unlike all the unconventional superconductors known so far, including TBLG, TMDs can be easily obtained by several methods (molecular beam epitaxy, carbon vapor deposition, atomic layer deposition, exfoliation, etc.), to yield scalable 2D superconductors of simple handling and transfer.

Among 2D TMD superconductors, single-layer $NbSe_2$ has received the most attention and its superconducting properties have been extensively studied.[33,34] Monolayer $NbSe_2$ has a noncentrosymmetric crystal structure (point group D_{3h}) which enables a form of spin orbit coupling (SOC) where spins lock out of the plane, leading to Ising superconductivity[31] with enhanced robustness to in-plane magnetic fields.[32] The absence of inversion also enables singlet–triplet mixing,[25,35] so far of unknown magnitude. More recently, transport experiments have revealed a twofold anisotropy of the superconducting state under in-plane magnetic fields, which has been interpreted in terms of a competing nematic superconducting instability.[36,37] In parallel, tunneling junction experiments also claimed the existence of a subleading triplet order parameter to explain the dependence of the gap to in-plane fields in the thin film limit.[38] These experiments suggest sizable electronic correlations as the origin of the competing pairing instabilities. In this work, by means of high-resolution scanning tunneling microscopy and spectroscopy (STM/STS) measurements at 340 mK, we have observed a collective mode univocally associated to superconductivity, which we attribute to a related competing triplet (f-wave) pairing channel. This finding strongly suggests that many-body correlations play a dominant role in the emergence of superconductivity among TMD superconductors.

2. Results

We investigate the superconducting properties of single-layer $NbSe_2$ with samples grown by molecular beam epitaxy on bilayer graphene on SiC(0001) and h-BN/Ir(111) substrates (see Supporting Information for details). Since the phenomenology is very similar on both substrates, in the following we will focus on the experiments on $NbSe_2$/graphene (see Supporting Information for data on h-BN). **Figure 1**a illustrates the typical morphology of our $NbSe_2$ monolayers on graphene. At low temperatures, single-layer $NbSe_2$ exhibits charge density wave

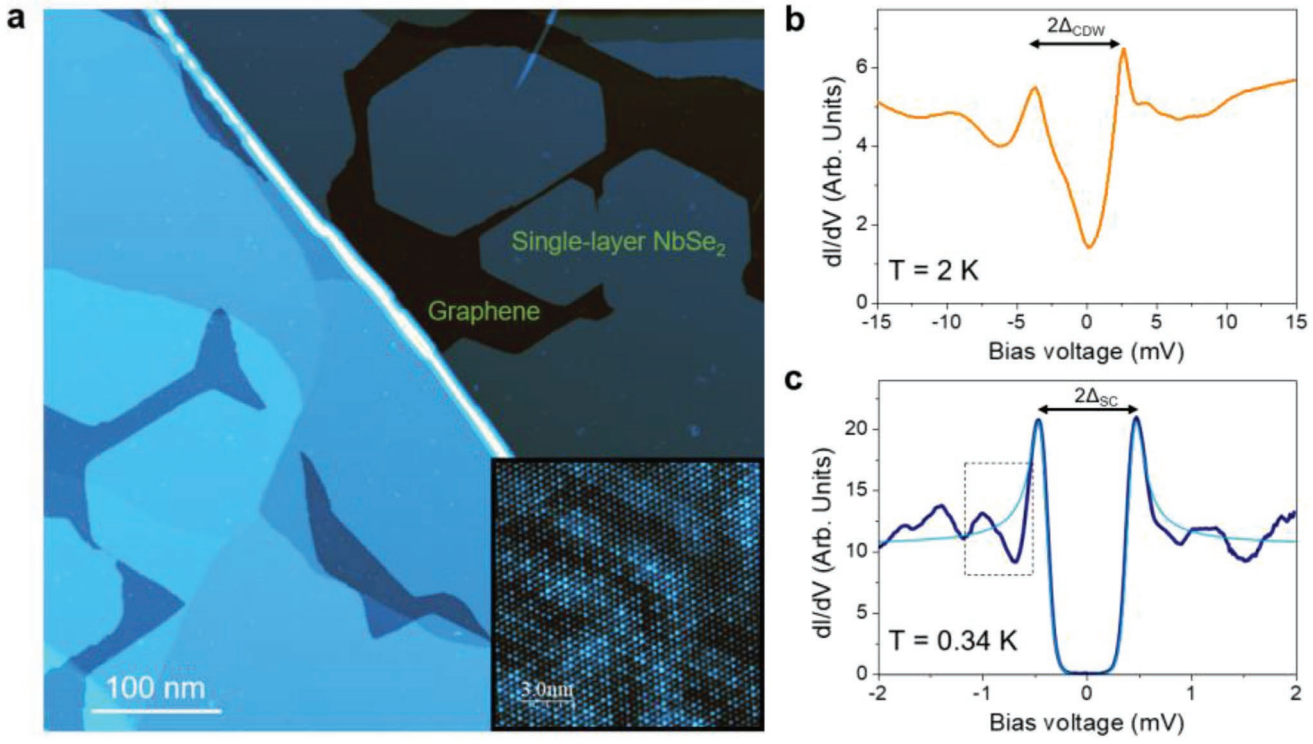

Figure 1. Low-energy electronic structure of single-layer $NbSe_2$. a) Large-scale STM image of single-layer $NbSe_2$/BLG/SiC(0001) in the submonolayer coverage range (V_s = 105 mV, I = 0.01 nA, T = 0.34 K). The inset shows an atomically resolved STM image of the $NbSe_2$ layer showing the 3 × 3 CDW order (V_s = 30 mV, I = 0.46 nA, T = 0.34 K). b,c) Low-bias STM dI/dV spectra acquired on single-layer $NbSe_2$ showing the CDW gap (Δ_{CDW}) (f = 833 Hz, $V_{a.c.}$ = 200 μV) in (b) and the superconducting gap (Δ) (f = 833 Hz, $V_{a.c.}$ = 20 μV) in (c). The boxed region in (c) shows one of the characteristic dip–hump features found in this system.

(CDW) order and superconductivity with critical temperatures of $T_{CDW} \approx 33$ K and $T_C \approx 2$ K, respectively.[27,30] Both electronic phases develop a gap feature in the density of states (DOS) at the Fermi level (E_F) that can be measured via low-bias STS measurements. The CDW gap in the dI/dV spectra (Figure 1b) appears as a V-shaped dip at E_F bound by coherence peaks with average locations around ±3–5 mV (see ref. [27]) The CDW only gaps out a fraction of the Fermi surface, which allows the development of superconductivity at lower temperatures.

The fingerprint of the superconducting state in single-layer $NbSe_2$ is shown in Figure 1c, which displays a typical dI/dV curve acquired at $T = 0.34$ K. This spectrum reveals an absolute gap that fits the BCS gap of width $\Delta_{BCS} = 0.38$ meV (light blue curve). The averaged BCS gap over different locations is $\overline{\Delta_{BCS}} = 0.4$ meV. As can be seen, however, the experimental conductance for energies higher than the coherence peaks ($|V| > 0.6$ meV) departs from the BCS conductance and shows several dip–hump satellite features at both polarities, such as those shown in the dashed rectangle in Figure 1c. We note that these STS features are unique to single-layer $NbSe_2$, and are not present in bulk (see Supporting Information for STS in bulk $NbSe_2$).

To better describe these spectral features, **Figure 2**a shows four dI/dV curves taken in different locations. These curves reveal the existence of multiple dip–hump features (or peaks, see Supporting Information) at both polarities, which are seen usually symmetric with respect to E_F and nearly equidistant. We performed statistical analysis over 2855 dI/dV curves acquired at $T = 0.34$ K in different spatial locations, using several samples and tips (see Supporting Information). As seen in the histogram of Figure 2b, this analysis reveals the existence of three clear satellite peaks within $|V| = 3$ mV (both polarities exhibit similar statistics). A much weaker and wider fourth peak is also present in the histogram, but since its energy is already close to the CDW coherence peaks, we do not believe it to be a replica and, therefore, we do not consider it further.

The non-flat structure of the histogram along with the tip calibration procedures on Cu(111) and graphene (Supporting Information) enables to rule out tip effects as the origin for these peaks. The main energy values of the identified peaks ($\Omega_{n=1-3}$), as defined from the nearest coherence peak ($\Omega_n = E_n - \Delta$ with E_n the energy of the nth peak from E_F), appear to be in all cases multiple of the energy of the first peak, that is, $\Omega_n = n \times \Omega_1 = n \times 0.53$ meV. Therefore, it appears reasonable to interpret them as harmonics of the same mode Ω_1.

To further characterize the satellite features, we first study their temperature dependence. **Figure 3**a shows a representative dataset of the evolution of the Ω_1 and Ω_2 features as the temperature approaches $T_C \approx 2$ K. As seen, the amplitude of the peaks rapidly decays in all cases, to finally disappear at 1.4 K. Figure 3b shows that the temperature evolution of the normalized amplitude of the Ω_2 mode (measured from the conductance floor at 2 meV) for empty states (black dots). The amplitude decays faster than what would be expected from thermal broadening (black curve) and, therefore, their disappearance can also be attributed to the weakening of superconductivity itself, suggesting that the satellite peaks are intrinsic to the superconducting state. The disappearance of these features above T_C allows us to rule out other origins for these peaks unrelated to superconductivity such as band structure effects, extrinsic inelastic features, and electronic renormalization due to electron–phonon interactions.

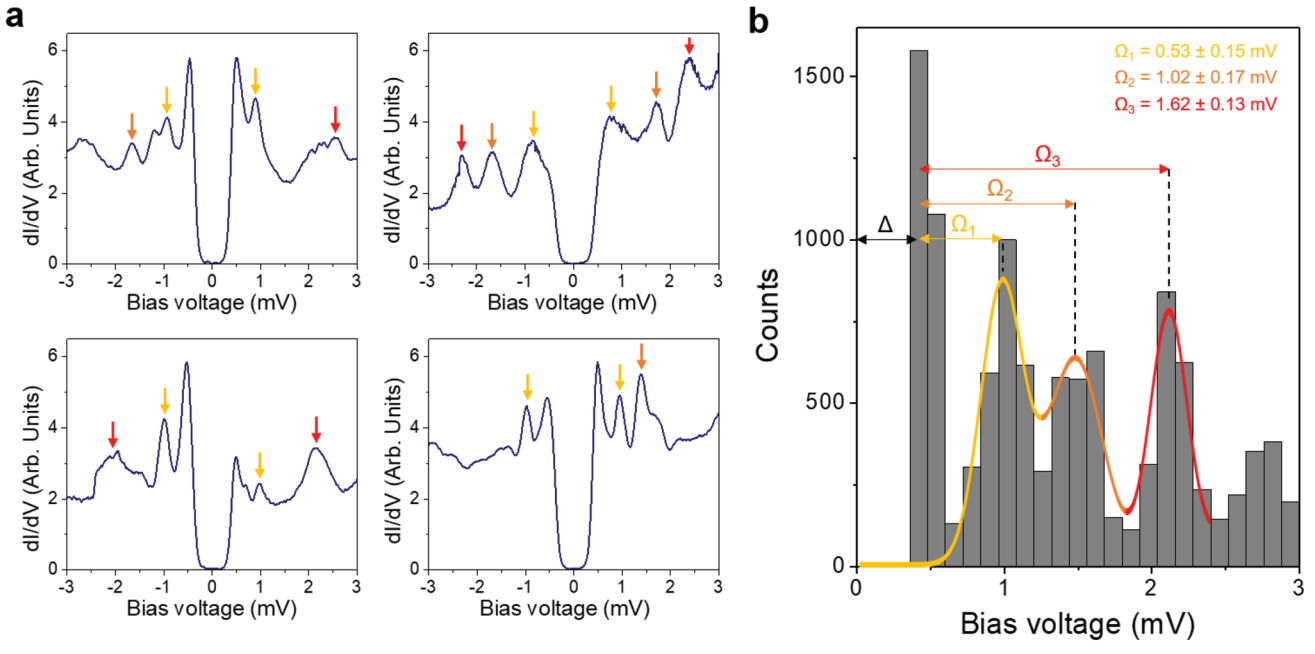

Figure 2. Statistical analysis of the STS dip–hump features. a) Four representative dI/dV curves acquired in single-layer $NbSe_2$ at $T = 0.34$ K. The arrows identify the fundamental Ω_1 mode (yellow) and the harmonics Ω_2 (orange) and Ω_3 (red). Parameters: $f = 833$ Hz, $V_{a.c.} = 20$ μV. b) Histogram of 2855 dI/dV curves acquired on different locations, and using different samples and tips. Three clear peaks can be identified for energies larger than the superconducting gap (Δ). A Gaussian fit to the peaks yield the following values: $\Omega_1 = 0.53$ meV, $\Omega_2 = 1.02$ meV and $\Omega_3 = 1.62$ meV.

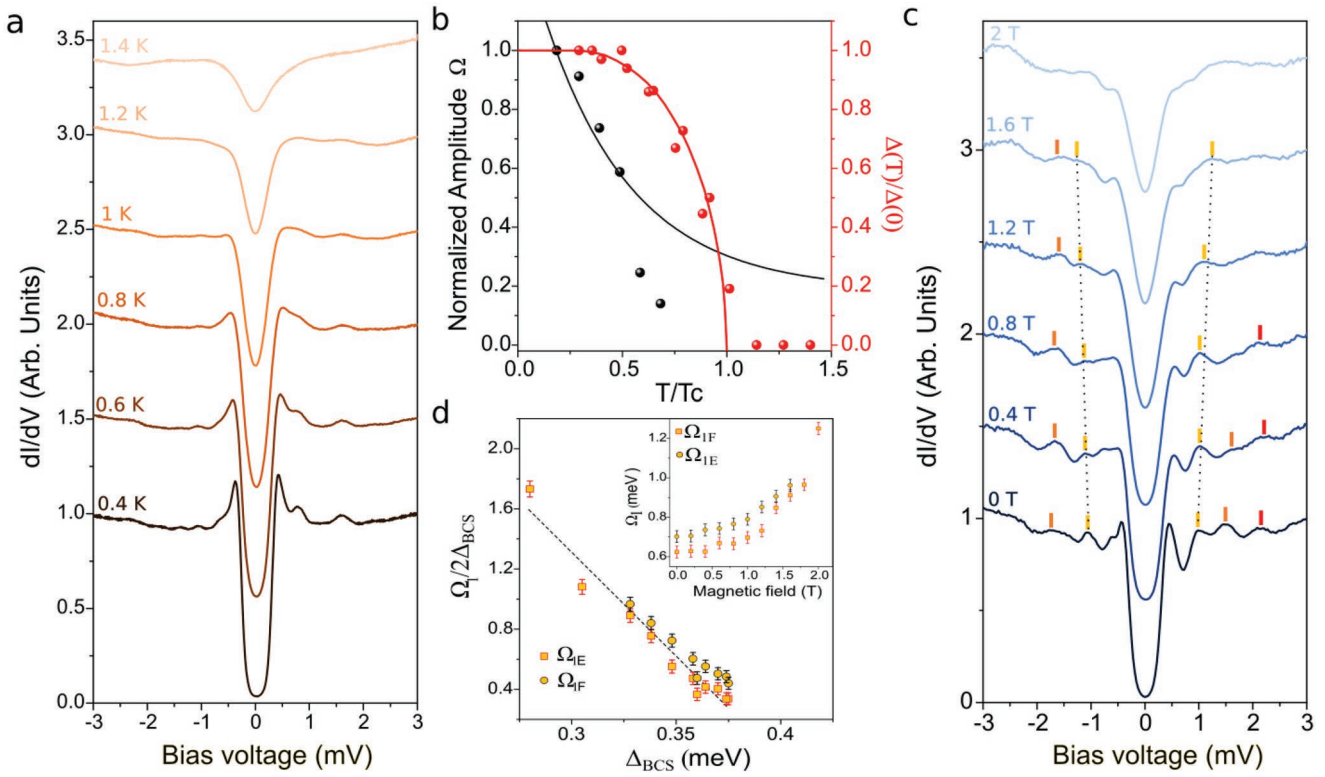

Figure 3. Temperature and magnetic field dependence of the bosonic modes. a) Evolution of the bosonic modes with temperature from 0.4 K up to 1.4 K ($f = 833$ Hz, $V_{a.c.} = 20$ μV). b) (black dots) Normalized amplitude of the Ω_2 mode for empty states in a, showing its decay with T below $T_C \approx 1.9$ K. The decay of amplitude of these STS features from thermal broadening (black curve) is shown to be slower with T. In red, the evolution of the measured Δ with T (circles, fitted to BCS) along with its T-dependence in the BCS theory (line). c) Dependence of the bosonic modes with the perpendicular magnetic field ($B_\perp$) up to 2 T ($f = 833$ Hz, $V_{a.c.} = 30$ μV). Marks indicate the maxima of the resonances and dashed lines connect the energy positions of the fundamental mode Ω_1. d) Ratio $\Omega_1/2\Delta$ versus Δ extracted from the $B_\perp$-evolution in (c) (Δ here is extracted from the BCS fit). Circles (squares) represent the filled (empty) states Ω_{1F} (Ω_{1E}). The dashed line is the linear fit. The inset illustrates the non-linear energy shift of the fundamental mode Ω_1 with the magnetic field.

Next, we examine the behavior of the satellite peaks under perpendicular magnetic field ($B_\perp$) at 0.34 K. Figure 3c shows a representative dataset of the evolution of the Ω_1, Ω_2, and Ω_3 features in clean regions of $NbSe_2$ for $B_\perp$ up to 2 T. Similar to the behavior observed in the T-dependence, these features gradually smear out with the strength of $B_\perp$ as superconductivity weakens and, ultimately, fade out within the mixed state. This further confirms the intrinsic relation between these satellite features and the superconducting state in single-layer $NbSe_2$. We also observe that the maxima of the satellite peaks shift toward higher energies as $B_\perp$ is increased. This is particularly evident for the fundamental mode Ω_1 at both polarities, which shifts in a non-linear fashion as shown in the inset of Figure 3d (see Supporting Information for the evolution of the SC gap).

A different way of quantifying the relation between Ω_n and Δ is to look at local spatial variations of the superconducting order parameter $\Delta(\vec{r})$, and whether they correlate with the local boson energy $\Omega_n(\vec{r})$, as both are accessible through STS measurements. In **Figure 4**, we show the correlation for the fundamental mode Ω_1 (yellow dots) and higher harmonics Ω_2 and Ω_3 (orange and red dots, respectively) from the set of dI/dV curves used to obtain the histogram of Figure 2b. As seen, all Ω_n modes exhibit an inverse correlation with respect to Δ with similar slope (black lines are the linear fits). This observation is consistent with the anticorrelation observed in the study of the $B_\perp$-dependence (Figure 3d). A further key insight is the fact that the majority of the values of the fundamental mode Ω_1 are smaller than 2Δ ($\Omega_1/2\Delta < 1$), in contrast to conventional superconductors where phonon-related features frequently lie beyond 2Δ, as in Pb with $\Omega_1/2\Delta \approx 1.7$ (see Supporting Information). The statistical confirmation that the fundamental mode has an energy below the pair breaking scale 2Δ implies that this mode cannot decay into fermionic quasiparticles and is therefore undamped, further supporting its interpretation as a superconducting collective mode.

To summarize our experimental evidence, the STS spectrum of superconducting monolayer $NbSe_2$ displays, in addition to the standard coherence peak at Δ, three satellite peaks at $\Omega_n = \Delta + n\Omega_1$ with $\Omega_1/2\Delta < 1$. These satellites gradually disappear with T and B as the superconducting state weakens, and their position shows a clear statistical anticorrelation between $\Omega_n/2\Delta$ and Δ. These observations are reproduced in two different substrates (graphene and h-BN), which allow us to rule out the potential role of the substrate in the formation of these STS features. Our findings are strong evidence for the presence of a collective mode of energy Ω_1 associated to the

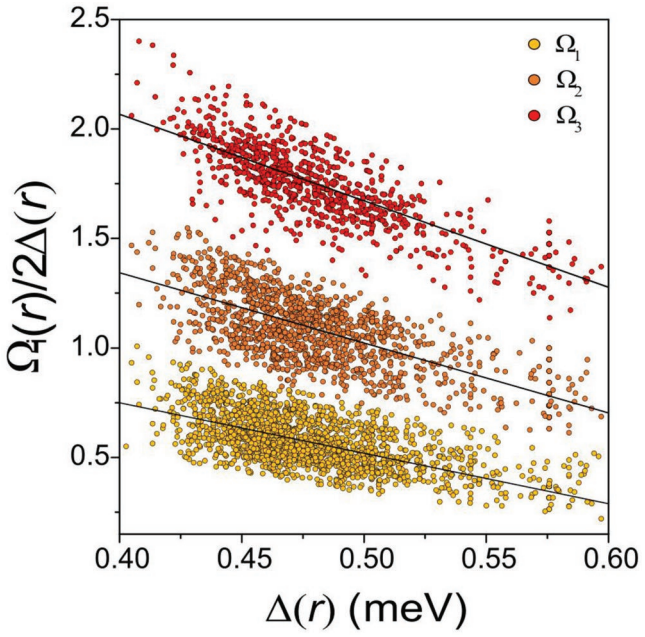

Figure 4. Local variations of the bosonic modes and the superconducting gap. Scatter plot of $\Omega/2\Delta$ against the superconducting gap (Δ) for the bosonic modes (Ω_1, Ω_2, and Ω_3), showing anticorrelation in all cases. The plot is obtained from the identification of the different Ω modes in 1974 dI/dV curves taken at $T = 0.34$ K in several samples, and using different calibrated STM tips. The black lines are fits for each subset of points. See SM for details regarding the analysis of the STS data.

superconducting state, which is coupled to fermionic quasiparticles and leaves its imprint in the tunneling spectra ($\propto$DOS). These observations have important implications regarding the nature of the pairing in this system, which we now discuss.

3. Theoretical Calculations

The existence of a collective mode can impact the spectral function in two ways, via elastic scattering (the renormalization of the electron self-energy due to virtual boson emission), which leads to a peak at $\Delta+\Omega_1$, as well as inelastic scattering (where quasiparticles might emit real bosons in the tunneling process) which leads to an onset-like feature. While the relative weight of these two contributions is system-dependent, the dip–hump shape of the satellite peaks observed in single-layer $NbSe_2$ closely resembles those features previously observed in strongly correlated superconductors, dominated by elastic scattering, rather than the typical shoulder-dip shape features of conventional superconductors induced by phonons (see the case of Pb(111) in Supporting Information) where both contributions can be comparable. Additionally, phonons cannot be responsible for our observed peak since there are none in the relevant energy range. In the high temperature phase without CDW, the phonon spectrum of single-layer $NbSe_2$ shows no relevant features below 3 meV (see refs. [26, 39]) and in the presence of the CDW, the lowest CDW phonon mode in the monolayer occurs at 70 cm^{-1} (8.6 meV).[40]

We therefore interpret our peaks as induced by elastic scattering from a collective mode intrinsic to the superconducting state, where two types of collective modes are possible. The first type belongs to excitonic fluctuations (or particle–hole modes), which become sharper after pairing due to the removal of decay channels into fermionic states. These modes might also be the mediators of the interaction that gives rise to superconductivity, or they may be detrimental for it, that is, pair breaking. A common example in many unconventional superconductors is a resonant magnetic excitation of spin-1[41] (an antiferromagnetic spin-wave) which is believed to mediate superconductivity[42] in cuprates[3–10], Fe-pnictides,[11–16] and heavy-fermion compounds.[20,21] Another known example are nematic fluctuations, as found in the Fe superconductors.[43] The second type are superconducting fluctuations (or particle–particle modes), most commonly due to close competition between pairing channels, like Leggett modes[44] in two-band superconductor MgB_2 or Bardarsis–Shrieffer (BS) modes[45] in Fe superconductors where s-wave and d-wave pairings are close competitors.[46] Either type of collective mode can be observed with different experimental techniques[47–49], including tunneling experiments, where bosonic modes are identified via the mentioned characteristic dip–hump features.[8,10,12,14,15,17–20] While these STS experiments are mostly interpreted in terms of particle–hole modes like spin-waves, there is no reason to preclude particle–particle modes to be found with this technique. Finally, all superconductors have an amplitude or Higgs mode, which is normally unobservable on its own[50], but it has been observed in bulk $NbSe_2$ due to its mixing with collective CDW modes.[51] Nevertheless, the Higgs mode can readily be discarded because in monolayer $NbSe_2$ the CDW mode has much higher energy than 2Δ and their coupling is highly suppressed.

Which of the previous collective mode scenarios applies to our experiment? Monolayer $NbSe_2$ has been predicted to be near a ferromagnetic instability[25,26] which competes with the CDW and, therefore, spin fluctuations could be sizable and potentially give rise to a particle–hole collective spin-wave. Such mode would indeed broaden and disappear as the temperature or magnetic field are increased to their critical values as observed in cuprates[47] and Fe-based materials.[48] Nevertheless, no magnetic order has been found in $NbSe_2$, and there is no direct evidence of strong spin fluctuations either. In the particle–particle scenario, however, there is a very natural mechanism for the emergence of collective modes: the competition between pairing channels signaled by the emergence of magnetic field-induced nematic superconductivity. To substantiate the characteristics of these collective modes, we now present a microscopic model of this competition which leads to explicit predictions that can be compared with our experiment.

$NbSe_2$ bands near the Fermi level are derived from the three t_{2g} Nb d orbitals, and consist of a hole pocket around the Γ point with dominant d_{z^2} character and hole pockets around the K points with $d_{x^2-y^2} \pm i d_{xy}$ character. This difference leads to strong Ising SOC for the K pockets but negligible SOC for the Γ pocket, and to different k-independent pairing channels: while both Γ and K pockets admit the standard s-wave state, the K points can also develop spin-triplet, orbital-singlet pairing of the $d_{x^2-y^2}$, d_{xy} orbitals which has f-wave symmetry.[52] For simplicity, we therefore assume the Γ pocket is a spectator

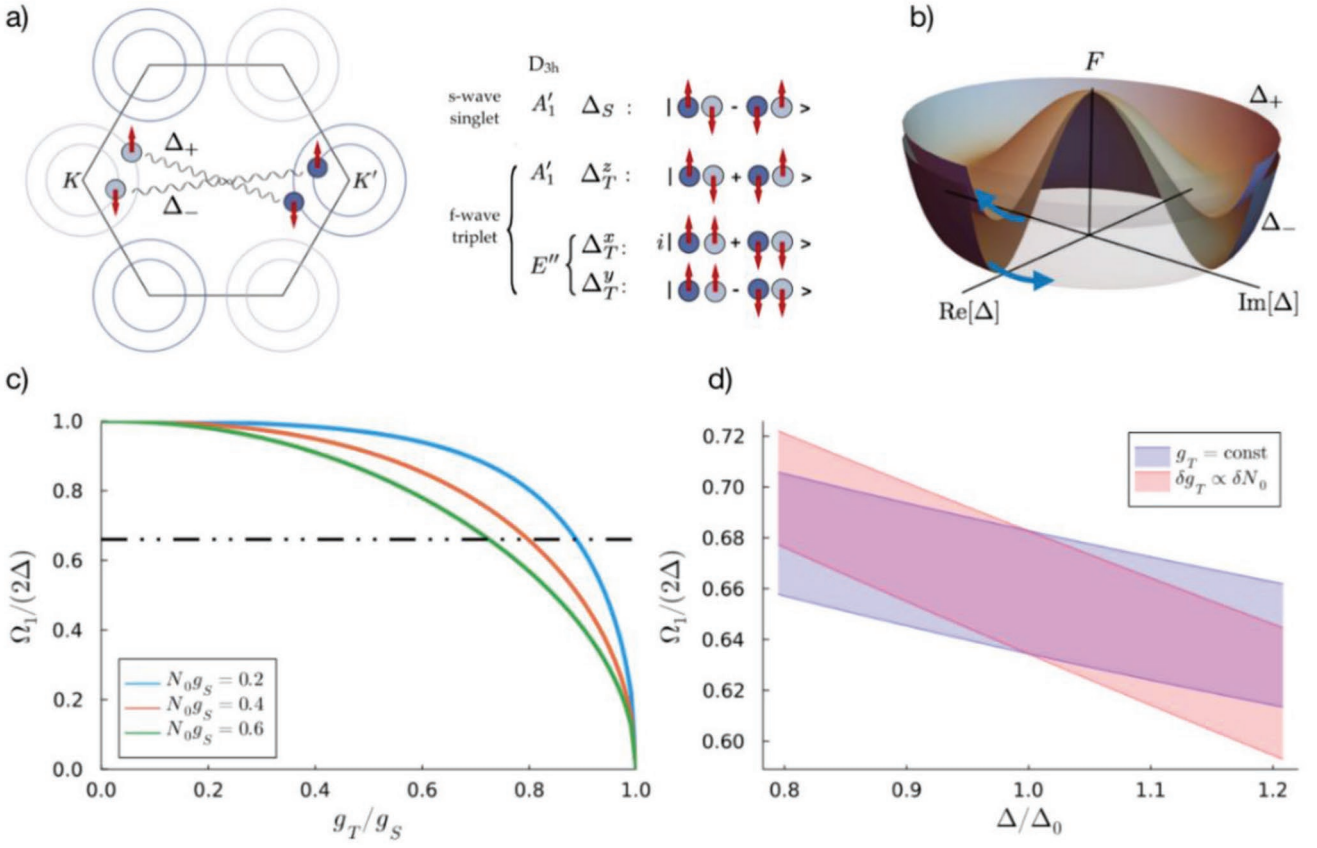

Figure 5. Pairing states and collective modes. a) Schematic Fermi surface near the *K* points and structure of the different pairing states considered. b) Schematic free energy for the gaps of the two spin-split Fermi surfaces, illustrating the Leggett mode as their relative phase fluctuation. c) Leggett mode energy normalized by the zero temperature gap $\Omega_1/2\Delta$ as a function of the ratio g_S/g_T. The collective mode is gapless when the two couplings are the same, and approaches 2Δ for vanishing triplet attraction $g_T = 0$. d) Allowed values of $\Omega_1/2\Delta$ when N_0 takes a range of values keeping g_S and g_T constant (blue), and when we additionally assume that g_T is correlated with N_0. Anticorrelation is generically observed but is more pronounced in the latter case.

with s-wave symmetry gap and use a model with just the K pockets

$$H_0(k) = \Psi^\dagger \left[\left(-\frac{k^2}{2m} - \mu \right) \tau_0 \sigma_0 + \lambda \tau_z \sigma_z \right] \Psi \tag{1}$$

where the τ_i and σ_i matrices act on the valley and spin index respectively, and λ is the Ising SOC. The pairing operators can be written as $\Delta_S = \Psi \tau_x i\sigma_y \Psi$ for the s-wave singlet which has A'_1 symmetry, and $\Delta_T^i = \Psi \tau_y \sigma_y \sigma_i \Psi$ with $i = x, y, z$ for the f-wave triplet, where Δ_T^z belongs to an A'_1 irrep while $\Delta_T^{x,y}$ make an E'' irrep (see **Figure 5**a for a schematic). In the presence of SOC, the mixing of the A'_1 singlet and A'_1 triplet becomes allowed. This mixing scales with the difference of the DOS of the spin-split pockets which is however very small. In our model with the leading *k*-independent SOC λ the DOS difference and the mixing actually vanish, and the only effect of λ is to disfavor the E'' state. Nevertheless, if attraction in the f-wave channel is sizable, its E'' part can naturally be induced with an in-plane magnetic field, which can explain the previous experiments proposing the competition of nematic[36,37] and triplet[38] pairing.

Assuming an s-wave ground state and vanishing singlet-triplet mixing, the imaginary fluctuations toward the two nearby f-wave triplets A'_1 and E'' represent two collective modes of the Bardarsis–Schriefer type. The fluctuation toward the E'' channel is likely unobservable in practice because $\lambda \gg \Delta$, which implies T_C for the E'' state will nearly vanish. We therefore consider only the fluctuation toward the A'_1 triplet. In the presence of singlet–triplet mixing, this second mode still exists but no longer has a well-defined Bardarsis–Schriefer character, because the gaps in the spin-split Fermi surfaces take the mixed form $\Delta_\pm = \Delta_S \pm \Delta_T^z$. This mode can alternatively be interpreted as the relative phase fluctuation of the $\Delta_\pm$ gaps, that is, a Leggett mode[53] (see Figure 5b), which we take as the leading candidate to explain our experiments.

To model the Leggett mode explicitly, we consider attractive interactions in the s-wave singlet and f-wave triplet channels as follows

$$V = g_S \Delta_S^+ \Delta_S + g_T \Delta_T^+ \Delta_T \tag{2}$$

with g_S, $g_T < 0$. As discussed in ref. [52], g_S might be thought of as induced by electron–phonon coupling, while g_T can have

contributions from both electron–phonon and Coulomb interactions, in particular through effective spin fluctuation.[25] Depending on whether $|g_S|$ or $|g_T|$ is largest, we have a ground state with dominant singlet or triplet character, and we assume $|g_S| > |g_T|$. The energy of the Leggett mode can be computed with this model (see Supporting Information) and is obtained from the implicit equation

$$\frac{\arcsin\left(\Omega_1/2\Delta\right)}{\sqrt{\left(2\Delta/\Omega_1\right)^2-1}} = \frac{1}{N_0|g_T|} - \frac{1}{N_0|g_S|} \tag{3}$$

From the measured value of $\Omega_1/2\Delta = 0.66$ we can estimate the ratio g_T/g_S and hence how close the triplet state is. This first requires an estimate of $N_0 g_S$. If we assume a weak coupling BCS limit, a gap of $\Delta \approx 0.4$ meV and a Debye frequency cutoff in the range of bulk estimates $\omega_D \approx 20$ meV (see ref. [54]), this corresponds to $N_0 g_S \approx 0.2$. However, since the ratio $(2\Delta)/(k_B T_c) \approx 4.9$ in our experiment would denote moderate to strong coupling, the value of $N_0 g_S$ is likely larger. Figure 5c displays the numerical solution of $\Omega_1/2\Delta$ as a function of g_T/g_S for $N_0 g_S = 0.2$–0.6, showing this produces a range $g_T/g_S = 0.7$–0.9. The triplet attraction must therefore be sizable, but still not enough to overcome the singlet attraction.

To show that this collective mode can in fact be observed in STS measurements, we have also computed the tunneling spectra due to the renormalization of the fermionic self-energy by this collective mode following ref. [55], showing that it indeed leads to a peak at $E_1 = \Omega_1 + \Delta$ (see Supporting Information). This calculation could be extended to higher orders to show the existence of harmonics at $E_n = \Omega_1 + n\Delta$ as well. A prediction of the absolute amplitude of the peaks is however beyond the scope of our calculation.

Our theory also allows to predict that the energy of the collective mode has a similar exponential dependence on temperature as the gap itself (see Supporting Information). Because of this, the collective mode energy should stay roughly constant in T for low T as we observe and only show deviations as it approaches $T \approx T_c$, where estimating the energy is prevented by our resolution. Similarly, the amplitude of the peak is rapidly suppressed near $T \sim T_c$ because the weight of this boson, computed as the residue of its propagator, scales $\propto \Delta^2$. In the presence of a magnetic field, the collective mode energy shows a significant rise, surpassing 2Δ even at moderate fields $B \approx 1$T. While a quantitative prediction for this would involve modeling the vortex mixed state, it is clear that this change cannot originate just from changes in the gap, and we conjecture that the magnetic field might reduce g_T by hardening spin fluctuations. Complementary probes of this collective mode are needed to better understand its behavior under magnetic fields.

To address the observed local anticorrelation with the gap, we assume that local variations of the model parameters lead to variations in the collective mode energy.[56] Figure 5d shows the predicted band of allowed energies for two different scenarios. First, we consider that N_0 varies spatially, leading to variations of Δ, while g_S and g_T are kept constant. Moderate anticorrelation is obtained in this case. If we further assume that g_T depends on the DOS, as it would be for example if it relied on spin-fluctuations, we see that a larger anticorrelation is attained. Analysis of other scenarios shows the anticorrelation is quite generic for this collective mode, while a detailed match with experiments will require exact knowledge of the origin of the spatial fluctuations. Overall, we believe our model supports our hypothesis that the observed mode is the Leggett mode due to proximity of f-wave triplet and provides a consistent picture for our observations.

4. Discussion

Finally, it is also interesting to compare the case of single-layer $NbSe_2$ with that of other superconductors where particle–hole magnetic resonances have been observed, where there is an empirical universal relation between resonance energy and the gap as $\Omega/2\Delta \approx 0.64$ over two orders of magnitude of Δ (see ref. [57]). In this context, single-layer $NbSe_2$ lies in the region of the smallest Ω's along with the heavy-fermion compounds[20,21] with a very similar value $\Omega_1/(2\overline{\Delta_{BCS}}) = 0.53/0.8 = 0.66$. Such intriguing similarity invokes further comparative investigation between particle–hole and particle–particle collective modes.

In summary, our results in single-layer $NbSe_2$ have unequivocally demonstrated the existence of a bosonic, undamped collective mode associated to the superconducting state, which we have interpreted as the fluctuations to a competing f-wave triplet channel. Our findings create exciting new opportunities for directly exploring unconventional superconductivity in a 2D material of simple synthesis, handling, and experimental analysis. We expect that this work will trigger active research in other simple 2D TMD superconductors, where competing superconducting channels and eventually triplet superconductivity could arise as well.

Supporting Information

Supporting Information is available from the Wiley Online Library or from the author.

Acknowledgements

W.W. and P.D. contributed equally to this work. The authors acknowledge fruitful discussions with Félix Ynduráin. The authors also thank Samuel Navas for providing bulk $NbSe_2$ crystals. M.M.U. acknowledges support by the ERC Starting grant LINKSPM (grant 758558) and the Spanish MINECO under grants no. PID2020-116619GB-C21. D.M.S. is supported by a FPU predoctoral contract from MEFP No. FPU19/03195. F.J. acknowledges funding from the Spanish MCI/AEI/FEDER through grant PGC2018-101988-B-C21 and from the Basque government through PIBA grant 2019-81.

Conflict of Interest

The authors declare no conflict of interest.

Data Availability Statement

The data that support the findings of this study are available from the corresponding author upon reasonable request.

Keywords

2D materials, collective modes, electronic structure, molecular beam epitaxy, superconductivity, transition metal dichalcogenides

Received: July 4, 2022
Revised: August 18, 2022
Published online:

[1] A. B. Migdal, *Sov. Phys. JETP* **1958**, *34*, 996.
[2] G. M. Eliashberg, *Sov. Phys. JETP-USSR* **1960**, *11*, 696.
[3] H. F. Fong, P. Bourges, Y. Sidis, L. P. Regnault, A. Ivanov, G. D. Gu, N. Koshizuka, B. Keimer, *Nature* **1999**, *398*, 588.
[4] H. He, P. Bourges, Y. Sidis, C. Ulrich, L. P. Regnault, S. Pailhès, N. S. Berzigiarova, N. N. Kolesnikov, B. Keimer, *Science* **2002**, *295*, 1045.
[5] S. Pailhès, Y. Sidis, P. Bourges, C. Ulrich, V. Hinkov, L. P. Regnault, A. Ivanov, B. Liang, C. T. Lin, C. Bernhard, B. Keimer, *Phys. Rev. Lett.* **2003**, *91*, 237002.
[6] S. Pailhès, C. Ulrich, B. Fauqué, V. Hinkov, Y. Sidis, A. Ivanov, C. T. Lin, B. Keimer, P. Bourges, *Phys. Rev. Lett.* **2006**, *96*, 257001.
[7] S. D. Wilson, P. Dai, S. Li, S. Chi, H. J. Kang, J. W. Lynn, *Nature* **2006**, *442*, 59.
[8] F. C. Niestemski, S. Kunwar, S. Zhou, S. Li, H. Ding, Z. Wang, P. Dai, V. Madhavan, *Nature* **2007**, *450*, 1058.
[9] Q. Li, M. Hücker, G. D. Gu, A. M. Tsvelik, J. M. Tranquada, *Phys. Rev. Lett.* **2007**, *99*, 067001.
[10] J. Zhao, F. C. Niestemski, S. Kunwar, S. Li, P. Steffens, A. Hiess, H. J. Kang, S. D. Wilson, Z. Wang, P. Dai, V. Madhavan, *Nat. Phys.* **2011**, *7*, 719.
[11] A. D. Christianson, E. A. Goremychkin, R. Osborn, S. Rosenkranz, M. D. Lumsden, C. D. Malliakas, I. S. Todorov, H. Claus, D. Y. Chung, M. G. Kanatzidis, R. I. Bewley, T. Guidi, *Nature* **2008**, *456*, 930.
[12] L. Shan, J. Gong, Y. L. Wang, B. Shen, X. Hou, C. Ren, C. Li, H. Yang, H. H. Wen, S. Li, P. Dai, *Phys. Rev. Lett.* **2012**, *108*, 227002.
[13] M. Liu, L. W. Harriger, H. Luo, M. Wang, R. A. Ewings, T. Guidi, H. Park, K. Haule, G. Kotliar, S. M. Hayden, P. Dai, *Nat. Phys.* **2012**, *8*, 376.
[14] S. Chi, S. Grothe, R. Liang, P. Dosanjh, W. N. Hardy, S. A. Burke, D. A. Bonn, Y. Pennec, *Phys. Rev. Lett.* **2012**, *109*, 087002.
[15] Z. Wang, H. Yang, D. Fang, B. Shen, Q. H. Wang, L. Shan, C. Zhang, P. Dai, H. H. Wen, *Nat. Phys.* **2013**, *9*, 42.
[16] W. Hong, L. Song, B. Liu, Z. Zeng, Y. Li, D. Wu, Q. Sui, T. Xie, S. Danilkin, H. Ghosh, A. Ghosh, J. Hu, L. Zhao, X. Zhou, X. Qiu, S. Li, H. Luo, *Phys. Rev. Lett.* **2020**, *125*, 117002.
[17] C. L. Song, Y. L. Wang, Y. P. Jiang, Z. Li, L. Wang, K. He, X. Chen, J. E. Hoffman, X. C. Ma, Q. K. Xue, *Phys. Rev. Lett.* **2014**, *112*, 057002.
[18] C. Liu, Z. Wang, S. Ye, C. Chen, Y. Liu, Q. Wang, Q. H. Wang, J. Wang, *Nano Lett.* **2019**, *19*, 3464.
[19] C. Chen, C. Liu, Y. Liu, J. Wang, *Nano Lett.* **2020**, *20*, 2056.
[20] N. K. Sato, N. Aso, K. Miyake, R. Shiina, P. Thalmeier, G. Varelogiannis, C. Geibel, F. Steglich, P. Fulde, T. Komatsubara, *Nature* **2001**, *410*, 340.
[21] C. Stock, C. Broholm, J. Hudis, H. J. Kang, C. Petrovic, *Phys. Rev. Lett.* **2008**, *100*, 087001.
[22] Y. Cao, V. Fatemi, S. Fang, K. Watanabe, T. Taniguchi, E. Kaxiras, P. Jarillo-Herrero, *Nature* **2018**, *556*, 43.
[23] Y. Nakata, K. Sugawara, R. Shimizu, Y. Okada, P. Han, T. Hitosugi, K. Ueno, T. Sato, T. Takahashi, *NPG Asia Mater.* **2016**, *8*, e321.
[24] M. Bonilla, S. Kolekar, Y. Ma, H. C. Diaz, V. Kalappattil, R. Das, T. Eggers, H. R. Gutierrez, M. H. Phan, M. Batzill, *Nat. Nanotechnol.* **2018**, *13*, 289.
[25] D. Wickramaratne, S. Khmelevskyi, D. F. Agterberg, I. I. Mazin, *Phys. Rev. X* **2020**, *10*, 041003.
[26] S. Divilov, W. Wan, P. Dreher, E. Bölen, D. Sánchez-Portal, M. M. Ugeda, F. Ynduráin, *J. Phys.: Condens. Matter* **2021**, *33*, 295804.
[27] M. M. Ugeda, A. J. Bradley, Y. Zhang, S. Onishi, Y. Chen, W. Ruan, C. Ojeda-Aristizabal, H. Ryu, M. T. Edmonds, H.-Z. Tsai, A. Riss, S.-K. Mo, D. Lee, A. Zettl, Z. Hussain, Z.-X. Shen, M. F. Crommie, *Nat. Phys.* **2016**, *12*, 92.
[28] Y. Chen, W. Ruan, M. Wu, S. Tang, H. Ryu, H. Z. Tsai, R. Lee, S. Kahn, F. Liou, C. Jia, O. R. Albertini, H. Xiong, T. Jia, Z. Liu, J. A. Sobota, A. Y. Liu, J. E. Moore, Z. X. Shen, S. G. Louie, S. K. Mo, M. F. Crommie, *Nat. Phys.* **2020**, *16*, 218.
[29] J. T. Ye, Y. J. Zhang, R. Akashi, M. S. Bahramy, R. Arita, Y. Iwasa, *Science* **2012**, *338*, 1193.
[30] Y. Cao, A. Mishchenko, G. L. Yu, E. Khestanova, A. P. Rooney, E. Prestat, A. V. Kretinin, P. Blake, M. B. Shalom, C. Woods, J. Chapman, G. Balakrishnan, I. V. Grigorieva, K. S. Novoselov, B. A. Piot, M. Potemski, K. Watanabe, T. Taniguchi, S. J. Haigh, A. K. Geim, R. V. Gorbachev, *Nano Lett.* **2015**, *15*, 4914.
[31] X. Xi, Z. Wang, W. Zhao, J.-H. Park, K. T. Law, H. Berger, L. Forró, J. Shan, K. F. Mak, *Nat. Phys.* **2016**, *12*, 139.
[32] E. Sohn, X. Xi, W. Y. He, S. Jiang, Z. Wang, K. Kang, J. H. Park, H. Berger, L. Forró, K. T. Law, J. Shan, K. F. Mak, *Nat. Mater.* **2018**, *17*, 504.
[33] K. Zhao, H. Lin, X. Xiao, W. Huang, W. Yao, M. Yan, Y. Xing, Q. Zhang, Z.-X. Li, S. Hoshino, J. Wang, S. Zhou, L. Gu, M. S. Bahramy, H. Yao, N. Nagaosa, Q.-K. Xue, K. T. Law, X. Chen, S.-H. Ji, *Nat. Phys.* **2019**, *15*, 904.
[34] C. Rubio-Verdú, A. M. García-García, H. Ryu, D. J. Choi, J. Zaldívar, S. Tang, B. Fan, Z. X. Shen, S. K. Mo, J. I. Pascual, M. M. Ugeda, *Nano Lett.* **2020**, *20*, 5111.
[35] L. P. Gor'kov, E. I. Rashba, *Phys. Rev. Lett.* **2001**, *87*, 037004.
[36] A. Hamill, B. Heischmidt, E. Sohn, D. Shaffer, K. T. Tsai, X. Zhang, X. Xi, A. Suslov, H. Berger, L. Forró, F. J. Burnell, J. Shan, K. F. Mak, R. M. Fernandes, K. Wang, V. S. Pribiag, *Nat. Phys.* **2021**, *17*, 949.
[37] C. Cho, L. Jian, H. Tianyi, N. Cheuk Yin, G. Yuxiang, L. Gaomin, H. Mingyuan, W. Ning, J. Schmalian, R. Lortz, arXiv:2003.12467, **2020**.
[38] M. Kuzmanovic, T. Dvir, D. LeBouef, S. Illic, D. Möckli, M. Haim, S. Kraemer, M. Khodas, M. Houzet, J. Meyer, M. Aprili, H. Steinberg, L. Quay, arXiv:2104.00328, **2021**.
[39] R. Bianco, L. Monacelli, M. Calandra, F. Mauri, I. Errea, *Phys. Rev. Lett.* **2020**, *125*, 106101.
[40] X. Xi, L. Zhao, Z. Wang, H. Berger, L. Forró, J. Shan, K. F. Mak, *Nat. Nanotechnol.* **2015**, *10*, 765.
[41] M. Eschrig, *Adv. Phys.* **2006**, *55*, 47.
[42] D. J. Scalapino, *Rev. Mod. Phys.* **2012**, *84*, 1383.
[43] V. K. Thorsmølle, M. Khodas, Z. P. Yin, C. Zhang, S. V. Carr, P. Dai, G. Blumberg, *Phys. Rev. B* **2016**, *93*, 054515.
[44] A. J. Leggett, *Prog. Theor. Phys.* **1966**, *36*, 901.
[45] A. Bardasis, J. R. Schrieffer, *Phys. Rev.* **1961**, *121*, 1050.
[46] F. Kretzschmar, B. Muschler, T. Böhm, A. Baum, R. Hackl, H. H. Wen, V. Tsurkan, J. Deisenhofer, A. Loidl, *Phys. Rev. Lett.* **2013**, *110*, 187002.
[47] P. Dal, H. A. Mook, G. Aeppll, S. M. Hayden, F. Doğan, *Nature* **2000**, *406*, 965.
[48] T. Chen, Y. Chen, D. W. Tam, B. Gao, Y. Qiu, A. Schneidewind, I. Radelytskyi, K. Prokes, S. Chi, M. Matsuda, C. Broholm, P. Dai, *Phys. Rev. B* **2020**, *101*, 140504(R).
[49] G. Blumberg, A. Mialitsin, B. S. Dennis, M. V. Klein, N. D. Zhigadlo, J. Karpinski, *Phys. Rev. Lett.* **2007**, *99*, 227002.
[50] P. B. Littlewood, C. M. Varma, *Phys. Rev. Lett.* **1981**, *47*, 811.

[51] M. A. Méasson, Y. Gallais, M. Cazayous, B. Clair, P. Rodière, L. Cario, A. Sacuto, *Phys. Rev. B: Condens. Matter Mater. Phys.* **2014**, *89*, 060503.
[52] D. Shaffer, J. Kang, F. J. Burnell, R. M. Fernandes, *Phys. Rev. B* **2020**, *101*, 224503.
[53] N. Bittner, D. Einzel, L. Klam, D. Manske, *Phys. Rev. Lett.* **2015**, *115*, 227002.
[54] V. Eremenko, V. Sirenko, V. Ibulaev, J. Bartolomé, A. Arauzo, G. Reményi, *Phys. C* **2009**, *469*, 259.
[55] A. Abanov, A. V. Chubukov, J. Schmalian, *J. Electron Spectrosc. Relat. Phenom.* **2001**, *117–118*, 129.
[56] A. V. Balatsky, J. X. Zhu, *Phys. Rev. B* **2006**, *74*, 094571.
[57] G. Yu, Y. Li, E. M. Motoyama, M. Greven, *Nat. Phys.* **2009**, *5*, 873.